

## VIEWPOINT

### Variety in the Metal–Metal Bond

J. D. Corbett ..... 3821–3822

Intermetallic Studies and Bonding Concepts

**Keywords:** Solid-state structures / Polar intermetallics / Zintl phases / Metal-metal interactions / Clusters



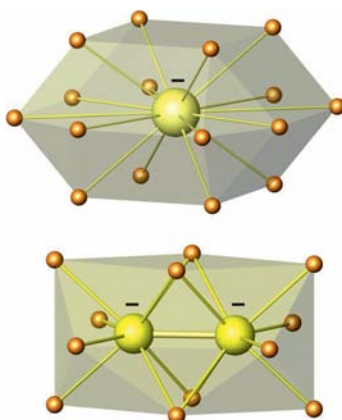
## MICROREVIEWS

### Metal Anions

M.-H. Whangbo,\* C. Lee,  
J. Köhler\* ..... 3841–3847

Metal Anions in Metal-Rich Compounds and Polar Intermetallics

**Keywords:** Intermetallic phases / Zintl anions / Electronic structure / Transition metal anions / Alkali metal anions



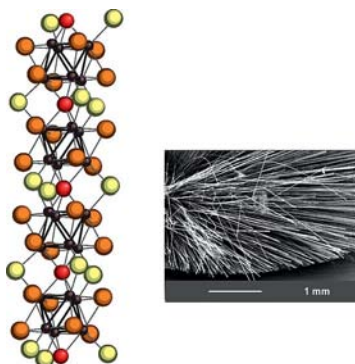
The electronic structures of metal-rich and intermetallic compounds containing alkali and transition metal anions are briefly reviewed. Transition metal anions exhibit bonding characteristics similar to those found for their main group analogues, because their *nd* orbitals act as reservoirs for holding ten electrons.

### Metal Cluster Chalcogenides

A. Perrin,\* C. Perrin\* ..... 3848–3856

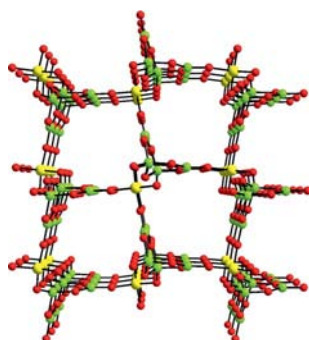
Low-Dimensional Frameworks in Solid State Chemistry of Mo<sub>6</sub> and Re<sub>6</sub> Cluster Chalcogenides

**Keywords:** Molybdenum / Rhenium / Cluster compounds / Chalcogenides / Solid state structure / Low-dimensional compounds



Mo<sub>6</sub> and Re<sub>6</sub> cluster chalcogenides built from the nanometric M<sub>6</sub>L<sub>14</sub> building blocks and synthesised by a solid-state route are reviewed and discussed. Access to 1D and 2D M<sub>6</sub> cluster frameworks depends on the various cluster units interconnections involving inner and/or apical ligands shared between adjacent units.

Open-framework boron oxides and metal borates can be prepared by the use of oxo boron clusters as building blocks. The synthesis, structures, and optical properties of these compounds are reviewed.



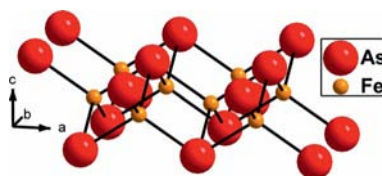
Z.-E. Lin, G.-Y. Yang\* ..... 3857–3867

Oxo Boron Clusters and Their Open Frameworks

**Keywords:** Microporous materials / Open frameworks / Borates / Clusters / Structure elucidation

## Iron Chalcogenide Superconductors

This review focuses on the structural aspects of newly discovered Fe-based pnictide and chalcogenide superconductors containing  $\text{FeX}_4$  tetrahedra ( $\text{X} = \text{As}$  and  $\text{Se}$ ) and revisits the popular  $\text{PbFCI}$ ,  $\text{ZrCuSiAs}$ , and  $\text{ThCr}_2\text{Si}_2$  structures. The oxypnictide tetrahedra are distorted and extended in an edge-sharing fashion.



A. K. Ganguli,\* J. Prakash .... 3868–3876

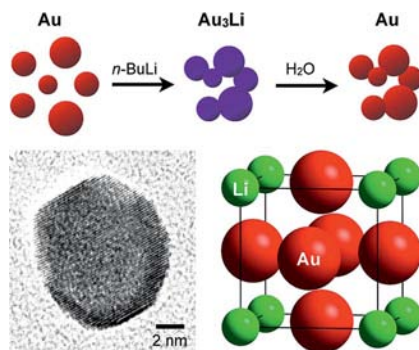
Iron-Based Superconductors with Extended  $\text{FeX}_4$  ( $\text{X} = \text{As}$  and  $\text{Se}$ ) Tetrahedra

**Keywords:** Iron / Pnictides / Chalcogens / Superconductors / Intermetallic compounds

## SHORT COMMUNICATIONS

### Polar Intermetallic Nanoparticles

Colloidal Au nanoparticle seeds react with *n*-butyllithium to form colloidal nanoparticles of  $L1_2$ -type  $\text{Au}_3\text{Li}$ . This compound represents a prototype binary polar intermetallic compound containing a highly electropositive element. Reaction with water decomposes  $\text{Au}_3\text{Li}$ , regenerating Au.



J. F. Bondi, R. E. Schaak\* ..... 3877–3880

Solution Chemistry Synthesis of Intermetallic Gold–Lithium Nanoparticles


**Keywords:** Gold / Lithium / Nanoparticles / Intermetallic phases

### Thiometalates

A polar indium thioantimonate  $[\text{Ni}(\text{en})_3][\text{InSbS}_4]$  (**1**) has been solvothermally synthesized. Its structure features a left-handed helical anionic chain of  $[\text{InSbS}_4]_n^{2n-}$  built upon trinuclear heterometallic clusters of  $\{\text{In}_2\text{SbS}_8\}$  as secondary building units. The thermal stability, optical and ferroelectric properties, as well as theoretical band structure and density of states have been studied.



M.-L. Feng, P.-X. Li, K.-Z. Du, X.-Y. Huang\* ..... 3881–3885

$[\text{Ni}(\text{en})_3][\text{InSbS}_4]$ : A One-Dimensional Polymeric Indium Thioantimonate with a Polar Structure 

**Keywords:** Indium / Antimony / Sulfur / Non-centrosymmetric compounds / Structure elucidation

# CONTENTS

## FULL PAPERS

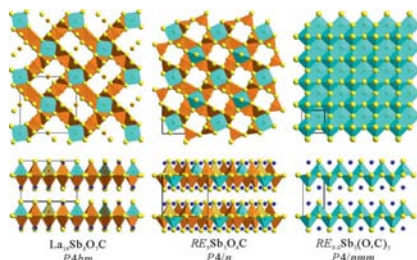
### Rare Earth Antimonide Oxycarbides

P. Wang, S. Forbes,  
V. Svitlyk, A. Aushana,  
Y. Mozharivskyj\* ..... 3887–3895



Resolving Composition and Structure of  $RE-Sb-O-C$  Natural Superlattice Phases ( $RE = La, Ho$ )

**Keywords:** Solid-state structures / Solid-phase synthesis / Rare earths



A series of  $RE-Sb-O-C$  oxycarbides were synthesized. These phases are natural superlattices based on rare earth antimonide and rare earth oxycarbide building blocks. The effects of carbon amount, rare earth metal purity, and annealing temperature on the stability and structure of these phases have been explored.

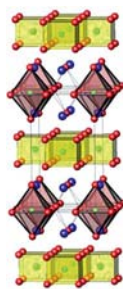
### Rare-Earth Cobalt Gallides

B. R. Slater, H. Bie, M. W. Gaultois,  
S. S. Stoyko, A. Mar\* ..... 3896–3903



Rare-Earth Cobalt Gallides  $RE_4Co_3Ga_{16}$  ( $RE = Gd-Er, Y$ ): Self-Interstitial Derivatives of  $RE_2CoGa_8$

**Keywords:** Rare earths / Cobalt / Gallium / Intermetallic phases / Magnetic properties



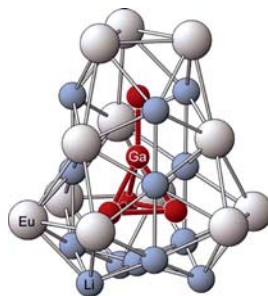
Co atoms enter available sites at the centres of octahedral  $Ga_6$  clusters in the parent  $RE_2CoGa_8$  structure to form self-interstitial derivatives,  $RE_4Co_3Ga_{16}$ .

### Gallium Clusters

A. Fedorchuk, Y. Prots, W. Schnelle,  
Y. Grin\* ..... 3904–3908

Bell-Like  $[Ga_5]$  Clusters in  $Eu_3Li_{5+x}Ga_{5-x}$  ( $x = 0.15$ )

**Keywords:** Cluster compounds / Gallium / Intermetallic phases / Electronic density of states



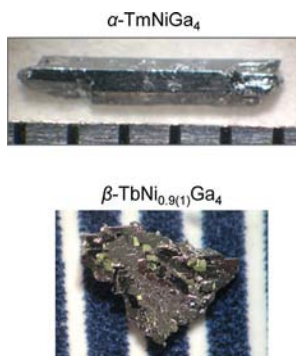
A new type of discrete bell-like  $[Ga_5]$  unit is found in the ternary gallide  $Eu_3Li_{5+x}Ga_{5-x}$  [space group  $R3m$ , Pearson symbol  $hR78$ ,  $a = 9.4859(5) \text{ \AA}$ ,  $c = 21.882(2) \text{ \AA}$ ,  $V = 1705.2(3) \text{ \AA}^3$ ]. The crystal structure is represented as  $[Eu^{2+}]_3[Li^+]_5[(1b)Ga^{4-}]_1[(3b)-Ga^{2-}]_3[(4b)Ga^{1-}]_1$  ( $xb$  = number of bonds, where  $x = 1-4$ ). The  $[Ga_n]$  clusters ( $n = 2-6$ ) present in gallium compounds of alkali, alkaline-earth metals or europium are compared.

### Lanthanide Polymorphs

M. C. Menard, B. L. Drake,  
G. T. McCandless, K. R. Thomas,  
R. D. Hembree, N. Haldolaarachchige,  
J. F. DiTusa, D. P. Young,  
J. Y. Chan\* ..... 3909–3919

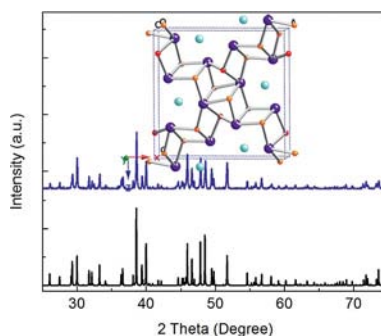
A Tale of Two Polymorphs – Growth and Characterization of  $\alpha-LnNiGa_4$  ( $Ln = Y, Gd-Yb$ ) and  $\beta-LnNi_{1-x}Ga_4$  ( $Ln = Tb-Er$ )

**Keywords:** Crystal growth / Magnetic properties / Intermetallic phases / Gallium



The single crystals of two polymorphs of  $LnNiGa_4$  were successfully grown by the flux growth method, namely, orthorhombic  $\alpha-LnNiGa_4$  ( $Ln = Y, Gd-Yb$ ) and, a new polymorph, tetragonal  $\beta-LnNi_{1-x}Ga_4$  ( $Ln = Tb-Er$ ). The physical properties of these polymorphs are reported in this paper.

A solid-state synthesis method was developed to make phase-pure  $\text{CaFe}_4\text{As}_3$ . Thermal stability studies were conducted on  $\text{CaFe}_4\text{As}_3$  and  $\text{CaFe}_2\text{As}_2$  over the 298–1473 K temperature range. Residual Sn on the surface of crystals reacts with crystals above 1173 K.  $\text{CaFe}_4\text{As}_3$  decomposes to give  $\text{CaFe}_2\text{As}_2$  and  $\text{Fe}_2\text{As}$ , and  $\text{CaFe}_2\text{As}_2$  forms  $\text{CaFe}_4\text{As}_3$  at high temperatures.

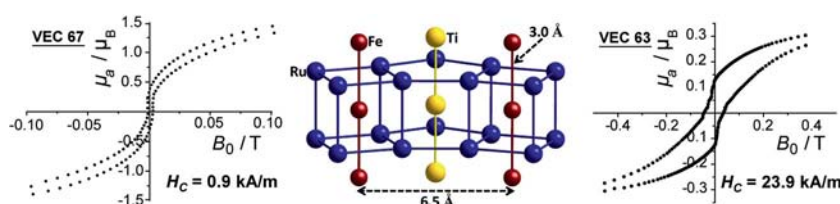


**T. Yi, A. P. Dioguardi, P. Klavins, N. J. Curro, L. L. Zhao, E. Morosan, S. M. Kauzlarich\*** ..... 3920–3925

Synthesis and Thermal Stability Studies of  $\text{CaFe}_4\text{As}_3$

**Keywords:** Calcium / Iron / Arsenic / Superconductors / Intermetallic phases / Solid-state reactions / Thermal stability

## Magnetic Borides



Chemically tuning the valence electrons (VE) of the boride series  $\text{Ti}_2\text{FeRu}_{5-n}\text{Rh}_n\text{B}_2$  between 67 and 63 induces the evolution from soft (67 VE,  $H_c = 0.9$  kA/m) to semi-hard (63 VE,  $H_c = 23.9$  kA/m) itinerant

ferromagnets. A section of the crystal structure (middle of the picture) shows the Fe–Fe interactions, which are mainly responsible for the ferromagnetic ordering observed at high temperatures.

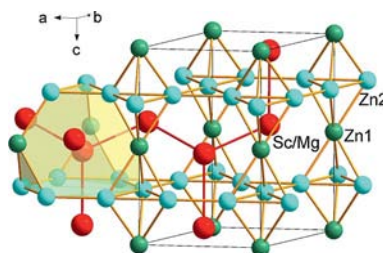
**B. P. T. Fokwa,\* H. Lueken, R. Dronskowski** ..... 3926–3930

Rational Design of Complex Borides – One-Electron-Step Evolution from Soft to Semi-Hard Itinerant Ferromagnets in the New Boride Series  $\text{Ti}_2\text{FeRu}_{5-n}\text{Rh}_n\text{B}_2$  ( $1 \leq n \leq 5$ )

**Keywords:** Borides / Magnetic properties / Transition metals / Intermetallic phases / Valence electron count

## Sc/Mg Alloys

Alloys between two isostructural binary phases do not always form solid solutions in the whole composition range, as observed for the pseudo-binary compound  $\text{Mg}_{1-y}\text{Zn}_y\text{Zn}_2$  that exhibits anisotropic lattice parameter changes as a response to Sc/Mg alloying. The Zn–Zn antibonding states at the Fermi energy appear to be the major driving force for the stabilization of the  $\text{ScZn}_2$  Laves phase at high pressure.

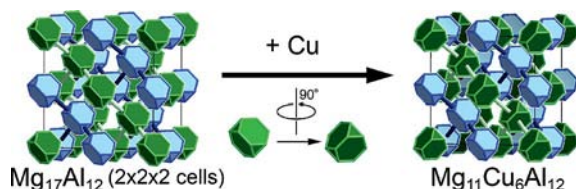


**W. Wang, G. Chen, Y. Wang, Q. Lin\*** ..... 3931–3935

$\text{Mg}_{1-y}\text{Sc}_y\text{Zn}_2$ : Limited Sc/Mg Alloying between Laves Phase  $\text{MgZn}_2$  and  $\text{ScZn}_2$  – What Drives  $\text{ScZn}_2$  into a High-Pressure Phase?

**Keywords:** Intermetallic phases / Solid-state reactions / Laves phases / Solid-state structures / Bonding

## Structural Chemistry



A supercell with a ( $90^\circ$ ) twist! The substitution of magnesium with copper atoms in  $\text{Mg}_{17}\text{Al}_{12}$  creates a  $2 \times 2 \times 2$  supercell adopted by  $\text{Mg}_{11}\text{Cu}_6\text{Al}_{12}$ , in which half of the  $\text{MgCu}_2$ -type clusters of the former are rotated by  $90^\circ$ . Relating the structures of

these phases to the simple, ubiquitous Laves phases through structural and quantum mechanical analysis leads to an explanation of the driving force for this structural transformation, and shows that complex structures can have simple origins.

**V. M. Berns, T. E. Stacey, M. Sapiro, D. C. Fredrickson\*** ..... 3936–3949

$\text{Mg}_{11}\text{Cu}_6\text{Al}_{12}$ , A New Link in the Structural Chemistry of  $\text{MgCu}_2$ -Type Clusters

**Keywords:** Solid-state structures / Structure elucidation / Intermetallic phases / Magnesium / Copper / Aluminium



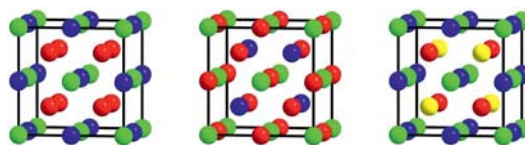
# CONTENTS

## Heusler Compounds

L. Basit, G. H. Fecher, S. Chadov,  
B. Balke,\* C. Felser ..... 3950–3954

Quaternary Heusler Compounds without  
Inversion Symmetry:  $\text{CoFe}_{1+x}\text{Ti}_{1-x}\text{Al}$  and  
 $\text{CoMn}_{1+x}\text{V}_{1-x}\text{Al}$

**Keywords:** Heusler compounds / Crystal  
structure / X-ray diffraction / Magnetic  
properties / Electronic structure



We report the quaternary Heusler compound derivatives  $\text{CoFe}_{1+x}\text{Ti}_{1-x}\text{Al}$  and  $\text{CoMn}_{1+x}\text{V}_{1-x}\text{Al}$  without centers of inversion. They were synthesized and their structure and magnetic properties investi-

gated.  $\text{CoMn}_{1+x}\text{V}_{1-x}\text{Al}$  ( $x > 0$ ) is a half-metallic ferrimagnet with its magnetic ground state controlled by the strong localized moment at the Mn atoms replacing V.

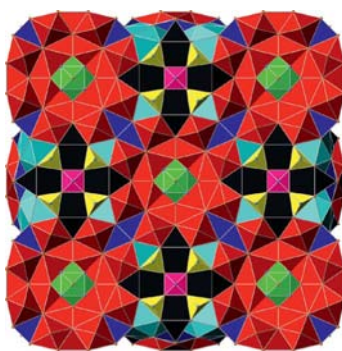
## Giant Magnetic Intermetallics

K. Kovnir, M. Shatruk\* ..... 3955–3962



Magnetism in Giant Unit Cells – Crystal  
Structure and Magnetic Properties of  
 $\text{R}_{117}\text{Co}_{52+\delta}\text{Sn}_{112+\gamma}$  ( $\text{R} = \text{Sm}, \text{Tb}, \text{Dy}$ )

**Keywords:** Intermetallic phases / Poly-  
hedra / Rare earths / Magnetic properties



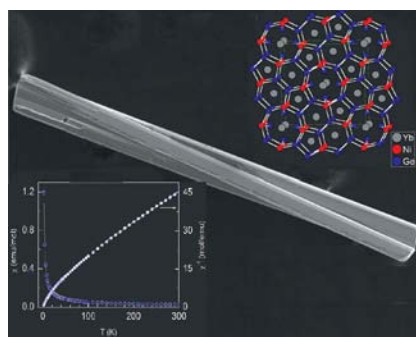
Compounds  $\text{R}_{117}\text{Co}_{52+\delta}\text{Sn}_{112+\gamma}$  exhibit a complex crystal structure with more than 1100 atoms in the unit cell. The structure can be deconvoluted into nested polyhedra that consist of shells of different polarity. Magnetic ordering of the rare-earth sublattice strongly depends on the nature of the  $\text{R}^{3+}$  ion, while the Co sublattice appears to be nonmagnetic.

## Magnetic Intermetallic Materials

S. C. Peter, S. Rayaprol, M. C. Francisco,  
M. G. Kanatzidis\* ..... 3963–3968

Crystal Structure and Properties of  
 $\text{Yb}_5\text{Ni}_4\text{Ge}_{10}$

**Keywords:** Rare earths / Intermetallic  
phases / Magnetic properties / Heat capacity / Ytterbium



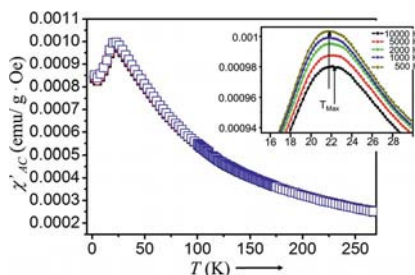
The new intermetallic compound  $\text{Yb}_5\text{Ni}_4\text{Ge}_{10}$  was obtained as single crystals in high yield from reactions run in liquid indium.  $\text{Yb}_5\text{Ni}_4\text{Ge}_{10}$  crystallizes in the  $\text{Sc}_5\text{Co}_4\text{Si}_{10}$  structure type in the tetragonal space group  $P4/mbm$ .  $\text{Yb}_5\text{Ni}_4\text{Ge}_{10}$  crystals show paramagnetic behavior with a lack of long-range magnetic ordering down to 2 K. The compound exhibits non-Fermi-liquid-like behavior at low temperatures.

## Semiconducting Antiferromagnet

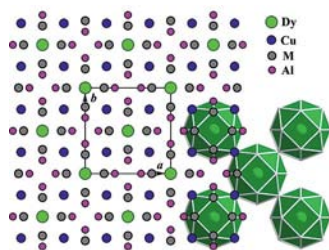
H. Djieutedjeu, J. P. A. Makongo,  
A. Rotaru, A. Palasyuk, N. J. Takas,  
X. Zhou, K. G. S. Ranmohotti, L. Spinu,  
C. Uher, P. F. P. Poudeu\* ..... 3969–3977

Crystal Structure, Charge Transport, and  
Magnetic Properties of  $\text{MnSb}_2\text{Se}_4$

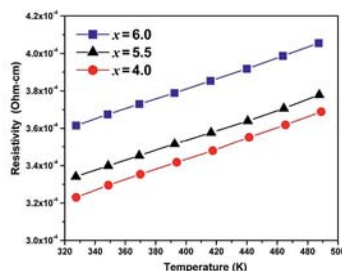
**Keywords:** Manganese / Antimony / Sel-  
enium / Semiconductors / Magnetic prop-  
erties / Thermoelectricity



The monoclinic  $\text{MnSb}_2\text{Se}_4$  phase is a narrow-gap p-type semiconductor that features isolated quasi-one-dimensional chains of edge-sharing  $\{\text{Mn}\}\text{Se}_6$  octahedra that run along  $[010]$ . Direct current (DC) and alternating current (AC) magnetic-susceptibility measurements strongly suggest that  $\text{MnSb}_2\text{Se}_4$  is not an ordinary antiferromagnet. The magnetism within individual chains in  $\text{MnSb}_2\text{Se}_4$  is rather controlled by competing interactions.



$\text{DyCu}_x\text{Al}_{12-x}$  ( $4.0 \leq x \leq 6.0$ ) features a 3D condensed network of Dy-centered, 20 vertex  $[\text{Al}_4\text{Cu}_8\text{M}_8]$  polyhedra, in which Cu/Al disorder has been observed on the  $M$  sites.



The metallic electrical conductivities decrease as  $x$  increases following the decreasing trend of the densities of states at the Fermi level.

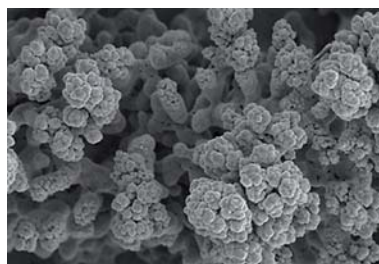
H. Lin, W.-Z. Cai, Y.-F. Shi,  
L. Chen\* ..... 3978–3983

Syntheses, Structure, Physical Properties, and Electronic Structures of  $\text{DyCu}_x\text{Al}_{12-x}$  ( $4.0 \leq x \leq 6.0$ )

**Keywords:** Solid state reactions / High temperature reactions / Intermetallic phases / Conducting materials / Rare earths / Dysprosium / Copper / Aluminium / Electronic structure / Magnetic properties

### Three-Dimensional Anodes

The effect of morphology and deposition substrate dimensionality has been studied for a series of lithium-ion battery anode structures. For  $\text{Cu}_2\text{Sb}$ -based anodes, enhanced cycling stability was found when a flat film was electrodeposited into a porous substrate to create a three-dimensional anode.



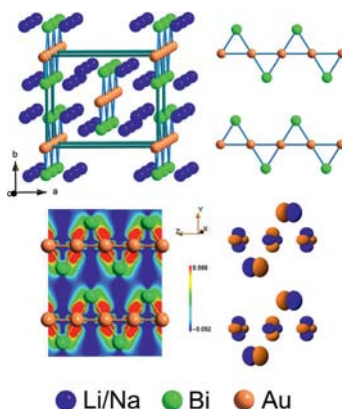
L. Trahey, H. H. Kung, M. M. Thackeray,  
J. T. Vaughan\* ..... 3984–3988

Effect of Electrode Dimensionality and Morphology on the Performance of  $\text{Cu}_2\text{Sb}$  Thin Film Electrodes for Lithium-Ion Batteries

**Keywords:** Electrochemistry / Thin films / Copper / Antimony / Intermetallic phases

### Zintl–Klemm Concept

The Au/Bi zigzag “ribbon” structural motif in  $\text{Na}_2\text{AuBi}$  is compared with the diamond-type Au/Bi and Tl/Tl networks in  $\text{Li}_2\text{AuBi}$  and  $\text{NaTl}$ . The “ribbon” is favoured when the alkali metal is large and valence  $d$  orbitals are actively involved in bonding.

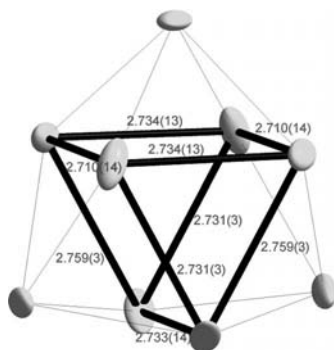


F. Wang, G. J. Miller\* ..... 3989–3998

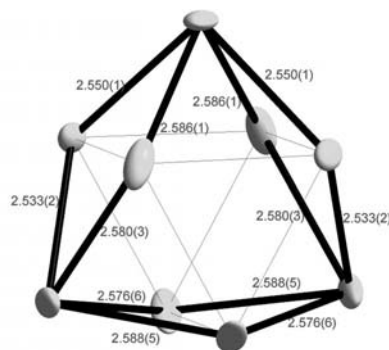
Revisiting the Zintl–Klemm Concept:  $\text{A}_2\text{AuBi}$  ( $\text{A} = \text{Li}$  or  $\text{Na}$ )

**Keywords:** Solid-state structures / Diamond network / Zintl phases / Zintl–Klemm formalism / Gold / Bismuth / Thallium / Alkali metals / Electronic structure / Density functional calculations

### Germanium Clusters



The first example of a fully ordered  $\text{Ge}_9^{2-}$  cluster was found in the low-temperature (100 K) structure of  $[\text{K}^+(2,2,2\text{-crypt})]_2\text{Ge}_9^{2-}$ . The room-temperature structure is trigonal and agrees very well with pre-



viously published reports, whereas the fully ordered low-temperature structure is monoclinic. The structural determination was complicated by extensive twinning.

J. Åkerstedt, S. Ponou, L. Kloo,  
S. Lidin\* ..... 3999–4005

Structural Investigation of a Fully Ordered  $\text{closo-Ge}_9^{2-}$  Cluster in the Compound  $[\text{K}^+(2,2,2\text{-crypt})]_2\text{Ge}_9^{2-}$

**Keywords:** Germanium / Zintl anions / Cluster compounds / X-ray diffraction / Cryptands

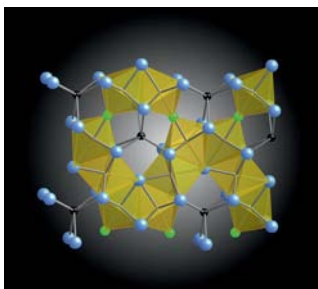
# CONTENTS

## Zintl Phase Hydrides

D. A. Lang,  
S. E. Lattner\* ..... 4006–4011

Two Germanide Hydride Phases Grown in Calcium-Rich Flux: Use of Interstitial Elements for Discovery of New Phases

**Keywords:** Zintl phases / Hydrides / Interstitials / Crystal growth / Flux growth



Reactions of germanium in Ca/Li flux produce two new phases owing to incorporation of hydride and oxide contaminants originally present in the flux metals. The structures of  $\text{LiCa}_7\text{Ge}_3\text{H}_3$  and  $\text{LiCa}_{11}\text{Ge}_3\text{OH}_4$  feature  $\text{Ge}^{4-}$  anions and hydride anions in octahedral coordination by calcium and lithium cations.

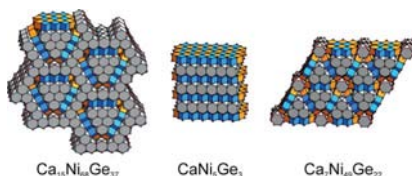
## Intermetallic Phases Ca-Ni-Ge

L. Siggelkow, V. Hlukhyi, B. Wahl,  
T. F. Fässler\* ..... 4012–4024



Complex Intermetallic Compounds:  $\text{CaNi}_5\text{Ge}_3$ ,  $\text{Ca}_{15}\text{Ni}_{68}\text{Ge}_{37}$ , and  $\text{Ca}_7\text{Ni}_{49}\text{Ge}_{22}$  – Three Multifaceted Ni-Ge Framework Structures Combining the Structural Motifs of  $\text{Ni}_3\text{Ge}$  and  $\text{CaNi}_2\text{Ge}_2$

**Keywords:** Intermetallic phases / Alloys / Germanides / Electron Localization Function / Structure elucidation



$\text{Ca}_{15}\text{Ni}_{68}\text{Ge}_{37}$ ,  $\text{CaNi}_5\text{Ge}_3$ , and  $\text{Ca}_7\text{Ni}_{48.9(4)}\text{Ge}_{22.1(4)}$  consist of complex networks of Ni and Ge atoms, which are based on two-dimensional slabs of the binary  $\text{Ni}_3\text{Ge}$  structure (yellow and blue polyhedra). As the Ca content decreases, the Ni-Ge substructures form one-, two-, and three-dimensional networks. These are separated by Ca atoms, which are at the center of the Ge/Ni hexagonal prisms (grey polyhedra).

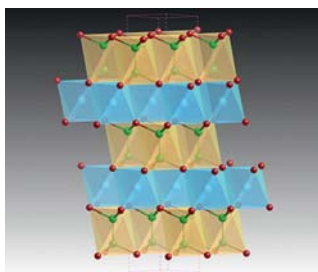
## Solid-State Structures

H. He, R. Stearrett, E. R. Nowak,  
S. Bobev\* ..... 4025–4036



Gallium Pnictides of the Alkaline Earth Metals, Synthesized by Means of the Flux Method: Crystal Structures and Properties of  $\text{CaGa}_2\text{Pn}_2$ ,  $\text{SrGa}_2\text{As}_2$ ,  $\text{Ba}_2\text{Ga}_5\text{As}_5$ , and  $\text{Ba}_4\text{Ga}_5\text{Pn}_8$  ( $\text{Pn} = \text{P}$  or  $\text{As}$ )

**Keywords:** Alkaline earth metals / Gallium / Pnictides / Solid-state structures / Density functional calculations



Six new alkaline earth metal gallium phosphides and arsenides have been synthesized for the first time. Their crystal structures have been established by single-crystal and synchrotron powder X-ray diffraction. Their electronic band structures have been determined by using DFT calculations, and their physical properties (e.g., electrical resistivity and thermopower) have been measured.

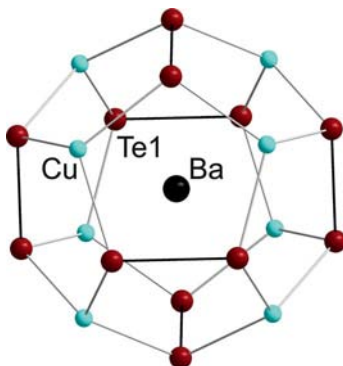
## Barium Copper Polychalcogenides

O. Mayasree, C. R. Sankar, Y. Cui,  
A. Assoud, H. Kleinke\* ..... 4037–4042



Synthesis, Structure, and Thermoelectric Properties of Barium Copper Polychalcogenides with Chalcogen-Centered Cu Clusters and  $\text{Te}_2^{2-}$  Dumbbells

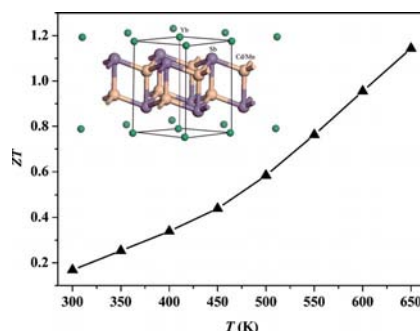
**Keywords:** Zintl phases / Solid-state structures / Sulfur / Selenium / Tellurium



These polychalcogenides are bestowed with Ba-centered pentagonal  $\text{Cu}_8\text{Te}_{12}$  dodecahedra and  $\text{Te}_2^{2-}$  dumbbells of full  $T_h$  symmetry, in addition to chalcogen-centered Cu clusters. In accord with the Zintl concept implying that these materials would be intrinsic semiconductors when  $x = 0$ , the Cu-deficient selenide-telluride with  $x = 0.3$  is a *p*-type semiconductor, exhibiting very low thermal conductivity.



The effects of substituting Cd by Mn in Zintl phases  $\text{YbCd}_{2-x}\text{Mn}_x\text{Sb}_2$  on their structure and thermoelectric properties are investigated. The presence of Mn reduces the cell parameters and electrical conductivity and enlarges the Seebeck coefficient, but it decreases the thermal conductivity simultaneously. The peak  $ZT$  of 1.14 at 650 K can be obtained when  $x = 0.15$ .



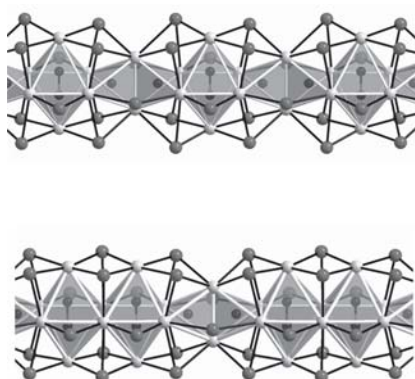
K. Guo, Q.-G. Cao, X.-J. Feng,  
M.-B. Tang, H.-H. Chen, X. Guo, L. Chen,  
Y. Grin, J.-T. Zhao\* ..... 4043–4048

Enhanced Thermoelectric Figure of Merit of Zintl Phase  $\text{YbCd}_{2-x}\text{Mn}_x\text{Sb}_2$  by Chemical Substitution

**Keywords:** Intermetallic phases / Thermoelectric properties / Zintl phases / Solid-state reactions / Chemical substitution

## Carbide Nitrides

Two types of cerium iodide carbide nitride rod structures are reported. The first, in  $\text{Ce}_8\text{I}_6(\text{C}_2)(\text{N})_2$  (**1**), is composed of alternating single  $(\text{Ce}_6\text{C})$  octahedra and double  $(\text{Ce}_4\text{N})_2$  tetrahedra,  $\frac{1}{2}[\text{oct}]$ , the second type of rods comprises double  $(\text{Ce}_6\text{C})_2$  octahedra and double  $(\text{Ce}_4\text{N})_2$  tetrahedra,  $\frac{1}{2}[\text{oott}]$ , and is observed in  $\text{Ce}_{12}\text{I}_{18}(\text{C}_2)_2(\text{N})_2$  (**2**). Compound **2** shows different degrees of disorder on the micro- and nanoscale.



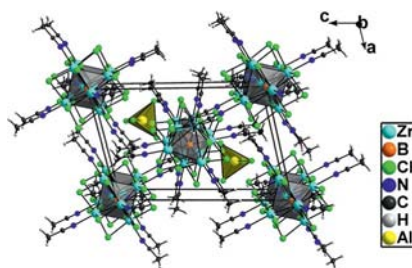
M. C. Schaloske, L. Kienle,  
Hj. Mattausch, V. Duppel,  
A. Simon\* ..... 4049–4056

Disorder in Rare Earth Metal Halide Carbide Nitrides

**Keywords:** Rod packing / Rare earths / Carbide nitrides / Disorder / X-ray diffraction / Electron microscopy

## Cationic Zirconium Clusters

Addition of Lewis acids  $\text{M}^{\text{III}}\text{Cl}_3$  ( $\text{M}^{\text{III}} = \text{Al}, \text{Ga}$  or  $\text{In}$ ) to acetonitrile solutions of molecular Zr cluster compounds, excised from  $\text{K}_2[(\text{Zr}_6\text{B})\text{Cl}_{15}]$ , shifts the chemical equilibria between different cluster species to the single product  $[(\text{Zr}_6\text{B})\text{Cl}_{12}(\text{CH}_3\text{CN})_6]^-[\text{M}^{\text{III}}\text{Cl}_4]^+$ .



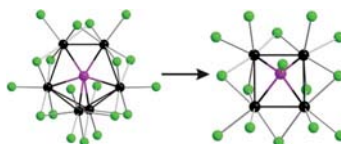
A. Bernsdorf,  
M. Köckerling\* ..... 4057–4062

Cationic Boron-Centred Hexanuclear Zirconium Cluster Compounds with Nitrilo Ligands and  $[\text{M}^{\text{III}}\text{Cl}_4]^+$  Counter Ions:  $[(\text{Zr}_6\text{B})\text{Cl}_{12}(\text{CH}_3\text{CN})_6][\text{M}^{\text{III}}\text{Cl}_4]^+$  with  $\text{M}^{\text{III}} = \text{Al}, \text{Ga}, \text{In}$

**Keywords:** Cluster compounds / Zirconium / Halides /  $^{11}\text{B}$  NMR spectroscopy / X-ray structure

## Tungsten Clusters

Solid-state reactions of highly reactive compounds or elements at low temperatures may provide a way to establish the potentially largest number of currently missing or unknown compounds. The reduction of  $\text{WCl}_6$  with elemental phosphorus yielded the phosphorus-centered  $\text{W}_6\text{PCl}_{17}$  cluster, which can be further reduced to yield the phosphinidene-capped cluster compound  $\text{W}_4(\text{PCl})\text{Cl}_{10}$ .



M. Ströbele, K. Eichele,  
H.-J. Meyer\* ..... 4063–4068

Phosphorus-Centered and Phosphinidene-Capped Tungsten Chloride Clusters

**Keywords:** Tungsten / Cluster compounds / Solid-state structures / X-ray diffraction



# CONTENTS

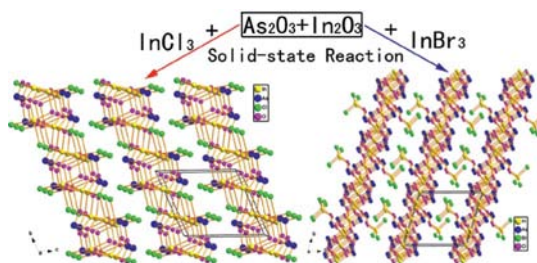
## Indium Arsenic Oxide Halides

X.-M. Jiang, Z.-N. Xu,  
Z.-Y. Zhao, S.-P. Guo, G.-C. Guo,\*  
J.-S. Huang ..... 4069–4076



Syntheses, Crystal Structures, and Optical Properties of Indium Arsenic(III) Oxide Halides:  $\text{In}_2(\text{As}_2\text{O}_5)\text{Cl}_2$  and  $\text{In}_4(\text{As}_2\text{O}_5)(\text{As}_3\text{O}_7)\text{Br}_3$

**Keywords:** Layered compounds / Indium / Arsenic / Halides / Optical properties



The first two indium arsenic(III) oxide halides,  $\text{In}_2(\text{As}_2\text{O}_5)\text{Cl}_2$  and  $\text{In}_4(\text{As}_2\text{O}_5)(\text{As}_3\text{O}_7)\text{Br}_3$ , which feature layered structures and three different indium-ion co-

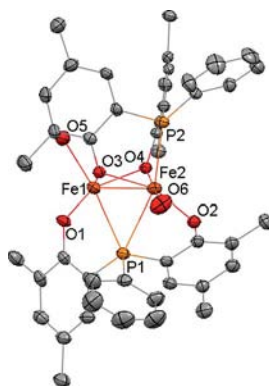
ordination geometries in one compound, were obtained by the solid-state reaction of  $\text{InCl}_3/\text{InBr}_3$ ,  $\text{As}_2\text{O}_3$ , and  $\text{In}_2\text{O}_3$ .

## Cluster Complexes

L.-C. Liang,\* Y.-N. Chang, H.-Y. Shih,  
S.-T. Lin, H. M. Lee ..... 4077–4082

Synthesis and Structural Characterization of Lithium and Iron Complexes Containing a Chelating Phenolate Phosphane Ligand

**Keywords:** Lithium / Iron / O,P ligands / Cluster compounds



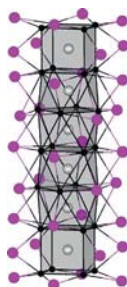
Biphenolate phosphane complexes of tetranuclear lithium and binuclear iron(II) were prepared and structurally characterized. The former, incorporating coordinated diethyl ether molecules, features a distinct structure, whereas the latter, with a diiron core bridged with two phenolate oxygen atoms and one phosphane, exhibits antiferromagnetic coupling between the two Fe centers.

## Cluster Complex Halides

M. Brühmann, A.-V. Mudring, M. Valldor,  
G. Meyer\* ..... 4083–4088

$\{\text{Os}_5\text{Lu}_{20}\}\text{I}_{24}$ , the First Extended Cluster Complex of Lutetium with Eight-Coordinate Endohedral Osmium Atoms in Two Different Environments

**Keywords:** Cluster compounds / Synthetic methods / Rare earths / Lutetium / Osmium / Electronic structure / Magnetic properties / Endohedral atoms



A 1D polar inter-metallic isolated by iodide: Square antiprisms and cubes of lutetium, in a surprising 4:1 ratio, sequester osmium atoms into a chain. The electronic structure features strong Os–Lu and Lu–I bonding interactions with lesser Lu–Lu and negligible Os–Os contributions resulting in a complicated magnetic cluster glass behavior.

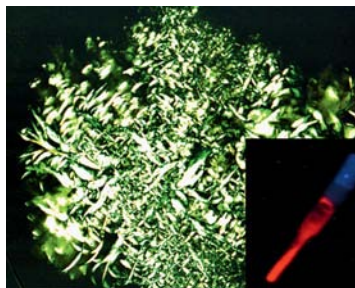
## Cluster Complex Halides

J. Bäcker, S. Mihm, B. Mallick, M. Yang,  
G. Meyer,\* A.-V. Mudring\* ..... 4089–4095

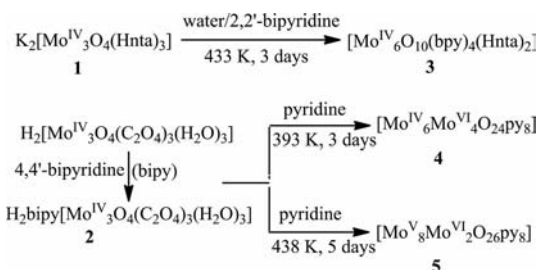


Crystalline and Liquid Crystalline Organic–Inorganic Hybrid Salts with Cation-Sensitized Hexanuclear Molybdenum Cluster Complex Anion Luminescence

**Keywords:** Cluster compounds / Ionic liquids / Liquid crystals / Luminescence / Synthesis design



The organic–inorganic hybrid salts  $[\text{C}_n\text{mim}]_2[\{\text{Mo}_6\}\text{Cl}_{14}]$  (mim = methylimidazolium) crystallize with  $n = 4$  and 6 and show thermotropic liquid-crystalline behaviour with  $n = 16$  and 18. Bright red luminescence, centred at around 730 nm, is observed either upon excitation of the imidazolium head group (475 nm) or the cluster-based levels (360 nm).



An unprecedented solvothermal treatment of triangular molybdenum(IV) oxo cluster compounds was established to prepare new oligonuclear oxomolybdenum clusters **3**, **4**,

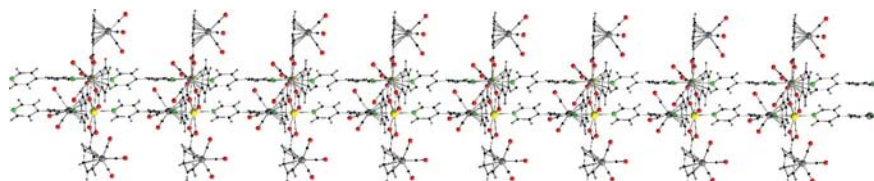
and **5**, providing a new approach for the synthesis of new types of molybdenum oxo clusters.

**J. Zhao, L. Xu\*** ..... 4096–4102

Solvothermal Treatment of Triangular Molybdenum(IV) Oxo Species – A New Approach for the Synthesis of New Molybdenum Oxo Clusters

**Keywords:** Molybdenum / Cluster compounds / Metal–metal interactions / Mixed-valent compounds / Solvothermal synthesis

## Coordination Polymers



The reaction of (benzoic acid)tricarbonylchromium [ $\{\eta^6\text{-C}_6\text{H}_5\text{COOH}\}\text{Cr}(\text{CO})_3$ ] with cadmium acetate with or without an-

cillary ligands in methanol or DMF leads to the formation of dinuclear and polymeric cadmium compounds.

**B. Murugesapandian, P. W. Roesky\*** ..... 4103–4108

Synthesis and Structures of Cadmium(II) Complexes with ( $\eta^6$ -Benzenecarboxylate)-tricarbonylchromium

**Keywords:** Cadmium / Chromium / Carbonyl ligands / Sandwich complexes / Coordination modes

\* Author to whom correspondence should be addressed.

Supporting information on the WWW (see article for access details).  
 This article is available online free of charge (Open Access).